Extension to Quadrilateral Element of Three Field Hu-Washizu Elasticity Formulation Based on Biorthogonal Systems

Bishnu P. Lamichhane, M.Pingaro, P.Venini

20 settembre 2016

1 Linear elastic continuum problem

In this section we briefly recovery the equations governing the linear elastic problem. The equilibrium equation is:

$$-\mathrm{div}(\boldsymbol{\sigma}) = \boldsymbol{f} \ , \tag{1}$$

while in small deformation is:

$$\boldsymbol{d} = \boldsymbol{\varepsilon}(\boldsymbol{u}) = \frac{1}{2}(\boldsymbol{\nabla}\, \boldsymbol{u} + \boldsymbol{\nabla}\, \boldsymbol{u}^T) \ . \tag{2}$$

In the case of linear elasticity we have:

$$\boldsymbol{\sigma} = \lambda\, tr(\boldsymbol{\varepsilon})\boldsymbol{I} + 2\mu\, \boldsymbol{\varepsilon} \tag{3}$$

where μ and λ are the Lamé constant. By some algebra one obtains:

$$\boldsymbol{\sigma} = \begin{pmatrix} \lambda(\varepsilon_{11} + \varepsilon_{22}) & 0 \\ 0 & \lambda(\varepsilon_{11} + \varepsilon_{22}) \end{pmatrix} + 2\mu \begin{pmatrix} \varepsilon_{11} & \varepsilon_{12} \\ \varepsilon_{12} & \varepsilon_{22} \end{pmatrix} , \tag{4}$$

and rearranging the equation (4):

$$\boldsymbol{\sigma} = \begin{pmatrix} (\lambda + 2\mu)\varepsilon_{11} + \lambda\, \varepsilon_{22} & 2\mu\, \varepsilon_{12} \\ 2\mu\, \varepsilon_{12} & (\lambda + 2\mu)\, \varepsilon_{22} + \lambda\, \varepsilon_{11} \end{pmatrix} . \tag{5}$$

2 Briefly introduction to modify Hu-Washizu

We define the trial variables: $\boldsymbol{\varepsilon}(\boldsymbol{u})$, $\boldsymbol{d}$ and $\boldsymbol{\sigma}$, while the test variables are: $\boldsymbol{\varepsilon}(\boldsymbol{v})$, $\boldsymbol{e}$ and $\boldsymbol{\tau}$.

$$-\int_\Omega \mathrm{div}(\boldsymbol{C} : \boldsymbol{d})) \cdot \boldsymbol{v} = \boldsymbol{f} \tag{6}$$

$$\begin{aligned} a((\boldsymbol{u}, \boldsymbol{d}), (\boldsymbol{v}, \boldsymbol{e})) + b((\boldsymbol{v}, \boldsymbol{e}), \boldsymbol{\sigma}) &= l(\boldsymbol{v}) && (7) \\ b((\boldsymbol{u}, \boldsymbol{d}), \boldsymbol{\tau}) &= 0 && (8) \end{aligned}$$

where:

$$\begin{aligned} a((\boldsymbol{u}, \boldsymbol{d}), (\boldsymbol{v}, \boldsymbol{e})) &= \int_\Omega \boldsymbol{d} : (\boldsymbol{C} : \boldsymbol{e})\, dx + \alpha \int_\Omega (\boldsymbol{\varepsilon}(\boldsymbol{u}) - \boldsymbol{d}) : (\boldsymbol{\varepsilon}(\boldsymbol{v}) - \boldsymbol{e})\, dx \ , && (9) \\ b((\boldsymbol{u}, \boldsymbol{d}), \boldsymbol{\tau}) &= \int_\Omega (\boldsymbol{\varepsilon}(\boldsymbol{u}) - \boldsymbol{d}) : \boldsymbol{\tau}\, dx \ . && (10) \end{aligned}$$

The modify weak formulation of the problem is:

$$
\begin{cases}
\alpha \int_\Omega (\boldsymbol{\varepsilon}(\boldsymbol{u}) - \boldsymbol{d}) : \boldsymbol{\varepsilon}(\boldsymbol{v})\, dx + \int_\Omega \boldsymbol{\varepsilon}(\boldsymbol{v}) : \boldsymbol{\sigma}\, dx & = \int_\Omega \boldsymbol{f} \cdot \boldsymbol{v}\, dx \\
\int_\Omega \boldsymbol{d} : \boldsymbol{C}\boldsymbol{e}\, dx - \alpha \int_\Omega (\boldsymbol{\varepsilon}(\boldsymbol{u}) - \boldsymbol{d}) : \boldsymbol{e}\, dx - \int_\Omega \boldsymbol{e} : \boldsymbol{\sigma}\, dx & = 0 \\
\int_\Omega (\boldsymbol{\varepsilon}(\boldsymbol{u}) - \boldsymbol{d}) : \boldsymbol{\tau}\, dx & = 0
\end{cases}
\tag{11}
$$

by rearranging:

$$
\begin{cases}
\alpha \int_\Omega \boldsymbol{\varepsilon}(\boldsymbol{u}) : \boldsymbol{\varepsilon}(\boldsymbol{v})\, dx - \alpha \int_\Omega \boldsymbol{d} : \boldsymbol{\varepsilon}(\boldsymbol{v})\, dx + \int_\Omega \boldsymbol{\varepsilon}(\boldsymbol{v}) : \boldsymbol{\sigma}\, dx & = \int_\Omega \boldsymbol{f} \cdot \boldsymbol{v}\, dx \\
-\alpha \int_\Omega \boldsymbol{\varepsilon}(\boldsymbol{u}) : \boldsymbol{e}\, dx + \int_\Omega \boldsymbol{d} : \boldsymbol{C}\boldsymbol{e}\, dx + \alpha \int_\Omega \boldsymbol{d} : \boldsymbol{e}\, dx - \int_\Omega \boldsymbol{e} : \boldsymbol{\sigma}\, dx & = 0 \\
\int_\Omega \boldsymbol{\varepsilon}(\boldsymbol{u}) : \boldsymbol{\tau}\, dx - \int_\Omega \boldsymbol{d} : \boldsymbol{\tau}\, dx & = 0
\end{cases}
\tag{12}
$$

It is possible to rewrite the system in equation (12) in matrix form in the following way:

$$
\begin{bmatrix}
\alpha \boldsymbol{A} & -\alpha \boldsymbol{B} & \boldsymbol{W} \\
-\alpha \boldsymbol{B}^T & \boldsymbol{K} + \alpha \boldsymbol{M} & -\boldsymbol{D} \\
\boldsymbol{W}^T & -\boldsymbol{D}^T & \boldsymbol{0}
\end{bmatrix}
\begin{bmatrix}
\boldsymbol{x}_u \\ \boldsymbol{x}_d \\ \boldsymbol{x}_\sigma
\end{bmatrix}
=
\begin{bmatrix}
\boldsymbol{b}_f \\ \boldsymbol{0} \\ \boldsymbol{0}
\end{bmatrix},
\tag{13}
$$

where $\boldsymbol{A} = \int_\Omega \boldsymbol{\varepsilon}(\boldsymbol{u}) : \boldsymbol{\varepsilon}(\boldsymbol{v})$, $\boldsymbol{B} = \int_\Omega \boldsymbol{d} : \boldsymbol{\varepsilon}(\boldsymbol{v})$, $\boldsymbol{W} = \int_\Omega \boldsymbol{\sigma} : \boldsymbol{\varepsilon}(\boldsymbol{v})$, $\boldsymbol{K} = \int_\Omega \boldsymbol{C}\boldsymbol{e} : \boldsymbol{d}$, $\boldsymbol{M} = \int_\Omega \boldsymbol{e} : \boldsymbol{d}$, $\boldsymbol{D} = \int_\Omega \boldsymbol{\sigma} : \boldsymbol{e}$. $\boldsymbol{D}$ is a diagonal matrix. Using this property it is possible condense statically $\boldsymbol{x}_d$ and $\boldsymbol{x}_\sigma$, and we obtain the following system in the only unknown $\boldsymbol{x}_u$:

$$
\left[\alpha \boldsymbol{A} - \alpha \left(\boldsymbol{B}\boldsymbol{D}^{-1}\boldsymbol{W}^{-T} + \boldsymbol{W}\boldsymbol{D}^{-1}\boldsymbol{B}^T\right) + \boldsymbol{W}\boldsymbol{D}^{-1}\left(\boldsymbol{K} + \alpha \boldsymbol{M}\right)\boldsymbol{D}^{-1}\boldsymbol{W}^T\right] \boldsymbol{x}_u = \boldsymbol{b}_f
\tag{14}
$$

3 Finite element discretization

We consider a quasi-uniform triangulation $\mathcal{T}_h$ of the polygonal domain Ω consists of simply, either quadrilateral or hexahedral. We take into account of standard bilinear finite element space $K_h \subset H^1(\Omega)$ defined on the triangulation $\mathcal{T}_h$, where:

$$
K_h := \left\{ v \in C^0(\Omega) : v_{|T} \in \mathcal{Q}_1(T),\ T \in \mathcal{T}_h \right\}, \quad K_h^0 = K_h \cap H_0^1(\Omega),
\tag{15}
$$

and the space of bubble functions

$$
B_h := \left\{ b_T \in H^1(T) : b_{T|\partial T} = 0 \text{ and } \int_T b_T\, dx > 0,\ T \in \mathcal{T}_h \right\},
\tag{16}
$$

and we define the spaces for strain and displacement as $\boldsymbol{S}_h := [K_h]^{2\times 2}$ and $\boldsymbol{V}_h := \left[K_h^0 \bigoplus B_h\right]^2$. In the next section we discuss the different choosing of bubble functions. For the discrete stress space we use:

$$
\boldsymbol{M}_h := \left\{ \boldsymbol{\tau}_h \in [M_h]^{2\times 2} : \int_\Omega \boldsymbol{\tau}_h : \boldsymbol{1}\, dx = 0 \right\} \subset \boldsymbol{S}_0\,,
\tag{17}
$$

and let $\{\phi_1, \cdots, \phi_n\}$ and $\{\mu_1, \cdots, \mu_n\}$ the n the basis functions for the space V_h and M_h respectively, we construct the functions μ_i using the following biorthogonality property between the space V_h and M_h:

$$
\int_\Omega \mu_i \phi_j\, dx = c_j \delta_{ij}\,, \quad c_j \neq 0\,, \quad 1 \leq i, j \leq n\,,
\tag{18}
$$

where δ_{ij} is Kronecker symbol, and c_j is a scaling factor which can be chosen to be proportion al to the area of support of ϕ_j. The local basis function of K_h and M_h for the reference square element (see figure 1) $\hat{T} := \{(x, y) : -1 \leq x \leq 1\,, -1 \leq y \leq 1\}$ are:

$$
\begin{aligned}
\phi_1 &= \frac{1}{4}(1-x)(1-y)\,, \quad \phi_2 = \frac{1}{4}(1+x)(1-y)\,, \\
\phi_3 &= \frac{1}{4}(1+x)(1+y)\,, \quad \phi_4 = \frac{1}{4}(1-x)(1+y)\,.
\end{aligned}
\tag{19}
$$

and

$$
\begin{aligned}
\mu_1 &= 1 - 3x - 3y + 9xy\,, \quad \mu_2 = 1 + 3x - 3y - 9xy\,, \\
\mu_3 &= 1 + 3x + 3y + 9xy\,, \quad \mu_4 = 1 - 3x + 3y + 9xy\,.
\end{aligned}
\tag{20}
$$

It is important to observe that the global basis functions of the space M_h are not continuous.

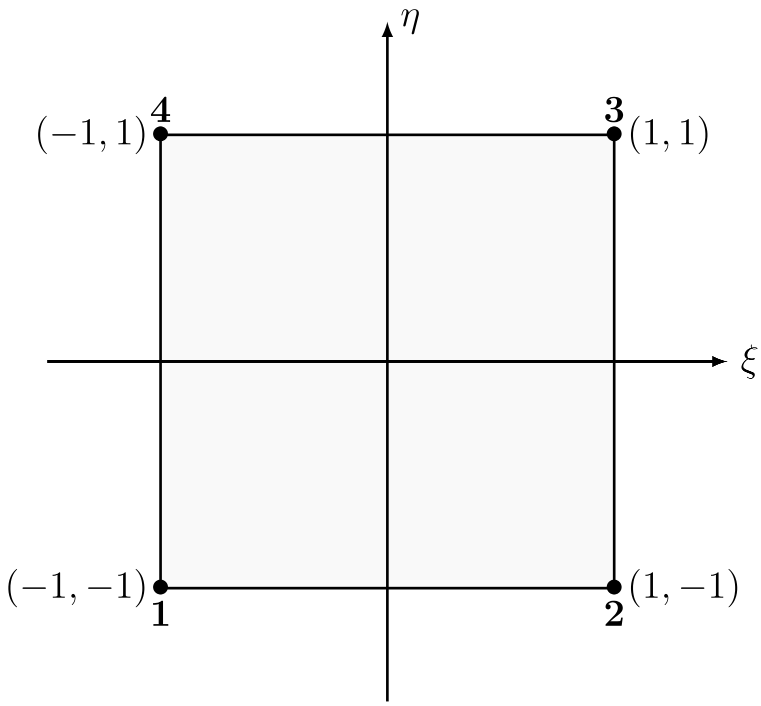

Figura 1: Reference Element

4 Bubble functions

In this section we detail the different choosing of the bubble functions. Addition of the bubble functions is essential to create a stable space. we have four types of bubbles. In the first two cases we use a modification of the standard bubble function ,that is for the reference element:

$$b_T(x,y) = (1-x^2)(1-y^2)\ , \tag{21}$$

while in the next two, we add to the standard bubble function another one.

4.1 One Bubble function (type 1)

As a first choice of bubble function we use:

$$\hat{b}_T(x,y) = c_T \cdot \phi_T(x,y) \cdot b_T(x,y)\ , \tag{22}$$

where c_T is a coefficient in order to obtain $\hat{b}_T(x_g, y_g) = 1$ (where $\boldsymbol{g}$ is the centroid of the elements), ϕ_K is the standard bilinear basis function corresponding to the lower-left corner of the square T. In the case of reference square element we obtain:

$$\hat{b}_T(x,y) = (1-x)(1-y)(1-x^2)(1-y^2)\ . \tag{23}$$

4.2 One Bubble function (type 2)

The second choice of bubble function we take:

$$\hat{b}_T(x,y) = c_T \cdot (a+bx+cy) \cdot b_T(x,y)\ , \tag{24}$$

where $a, b, c \in$ R and $a, b, c \neq 0$. For simplicity we set $a = b = c = 1$ and we obtain for the reference square:

$$\hat{b}_T(x, y) = (1 + x + y)(1 - x^2)(1 - y^2)\,. \tag{25}$$

4.3 Two Bubble functions

Using two bubble functions, where the first is the standard bubble function and the second bubble is a modification of the standard bubble:

$$\begin{aligned}\hat{b}_{T1}(x, y) &= b_T\,,\\ \hat{b}_{T2}(x, y) &= c_T \cdot (ax + by) \cdot b_T\,,\end{aligned} \tag{26}$$

where $a, b \in$ R and $a^2 + b^2 \neq 0$. For the sake of simplicity we adopt $a = b = 1$. One obtains:

$$\begin{aligned}\hat{b}_{T1}(x, y) &= (1 - x^2)(1 - y^2)\,,\\ \hat{b}_{T2}(x, y) &= (x + y)(1 - x^2)(1 - y^2)\,.\end{aligned} \tag{27}$$

4.4 Two Bubble functions, which one mixed

As a finally choice of bubbles we use a standard bubble function plus one mixed bubble function for the two components of displacement.

$$\begin{aligned}\hat{b}_{T1}(x, y) &= b_T\,,\\ \hat{b}_{T2,x}(x, y) &= (\nabla\phi_1)_x \cdot b_T\,,\\ \hat{b}_{T2,y}(x, y) &= (\nabla\phi_1)_y \cdot b_T\,,\end{aligned} \tag{28}$$

where $(\nabla\phi_1)_i$ is i-th component of the gradient of the first shape function ϕ. In this way we have as shape function for the displacement using the mixed bubble function the vector $\left[\hat{b}_{T2,x}(x, y), \hat{b}_{T2,y}(x, y)\right]$.

5 Numerical example

In this section we report some examples using the presented formulation to proven the good behaviour.

5.1 Square problem

First example is a unit square domain with homogeneous Dirichlet boundary conditions. The Lamé constant are fix to $\lambda = 123$ and $\mu = 79.3$. By imposition of the previously exact solution one obtain for the body force f

$$\begin{aligned}f_1 &= -\pi^2 \cos(\pi x)\sin(\pi y)\left(\lambda + \mu + 2\lambda\cos(\pi y) + 12\mu\cos(\pi y)\right),\\ f_2 &= -\pi^2 \sin(\pi x)\left(\lambda\cos(\pi y) + 3\mu\cos(\pi y) + 2\lambda\left(2\cos(\pi y)^2 - 1\right) + 2\mu\left(2\cos(\pi y)^2 - 1\right)\right)\end{aligned} \tag{29}$$

The exact solution is

$$u_1 = \cos(\pi x)\sin(2\pi y),\;\; u_2 = \sin(\pi x)\cos(\pi y). \tag{30}$$

The problem is study using two type of mesh: first of all using a square mesh and before using a trapezoidal mesh. The two types of mesh are shown in figures 2(a) and 2(b). Figures 3(a), 3(b), 4(a) and 4(b) shown the error in norm L^2 in the case of regular mesh for the different types of bubble functions used and types of coefficient α. All types of element converge in a good way. In Figures 5(a), 5(b), 6(a) and 6(b) we report the previously results in the case of trapezoidal meshes.

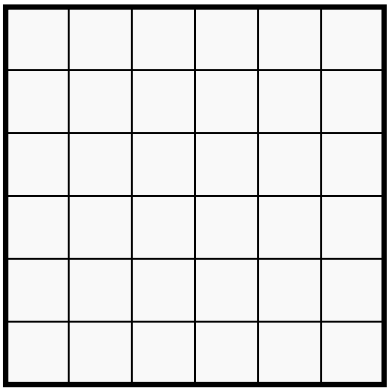

(a) Regular mesh

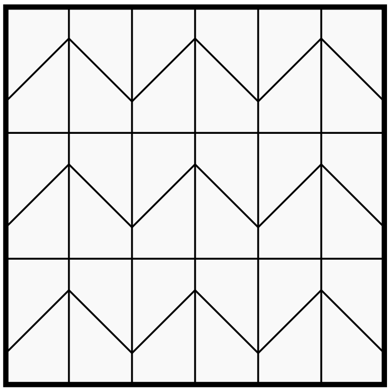

(b) Trapezoidal mesh

Figura 2: Square Problem

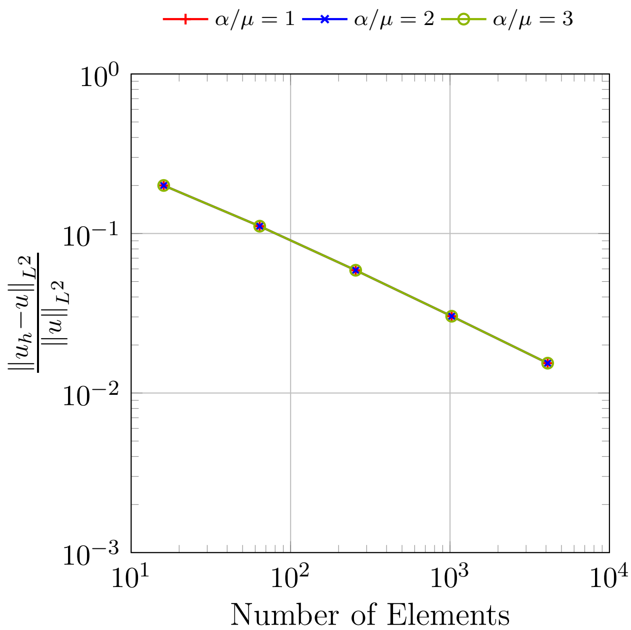

(a) type 1

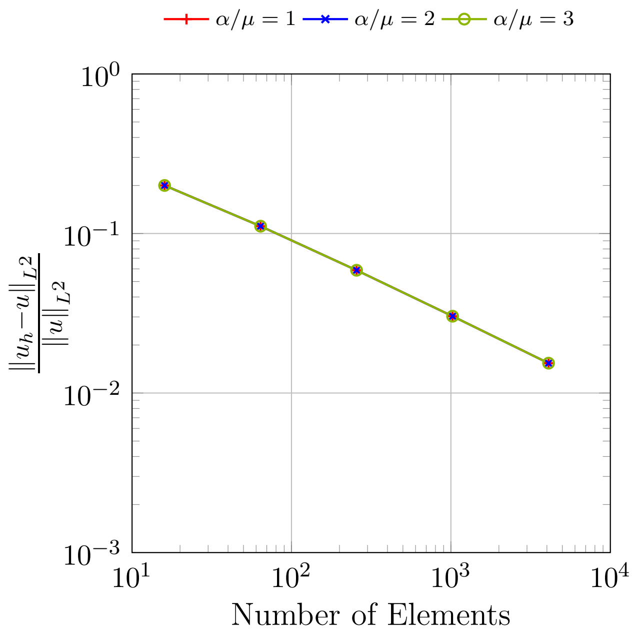

(b) type 2

Figura 3: The relative error vs. the number of elements measured relative to the L^2 norm (Case one bubble function and regular mesh)

5.2 Cantilever beam problem

Now we consider the beam with length $L = 10$ and height $l = 2$ as we shown in figure (). The Young modulus is set equal to $E = 1500$ and the Poisson $\nu = 0.4999$ and subjected to a distributed load as in figure 7 with $f = 300$. The exact solution is:

$$\begin{aligned} u(x, y) &= \frac{2f}{El}(1-\nu^2)x\left(\frac{l}{2} - y\right) , \\ v(x, y) &= \frac{f}{El}\left[x^2 + \frac{\nu}{1-\nu}\left(y^2 - ly\right)\right] . \end{aligned} \tag{31}$$

We use to model the beam two types of mesh: regular anf trapezoidal as in the previously example (see figures 2(a) and 2(b)). we shown in figures 10(a), 10(b), 11(a) and 11(b) the L^2-norm error for different

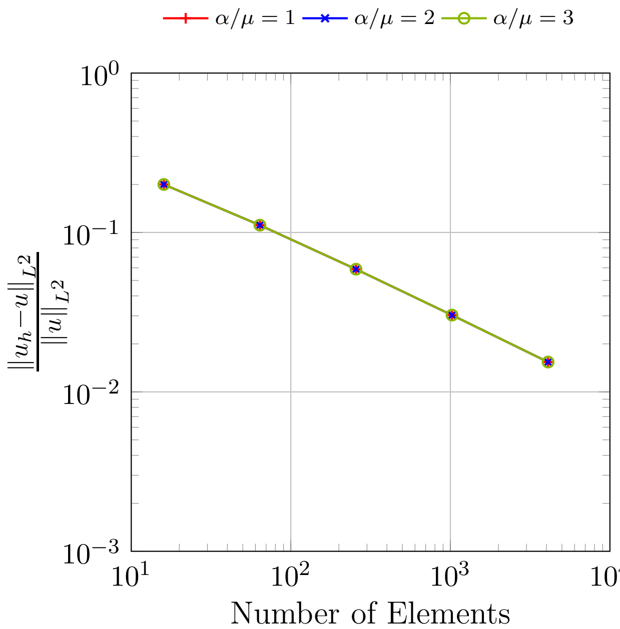

(a) Case two bubble function

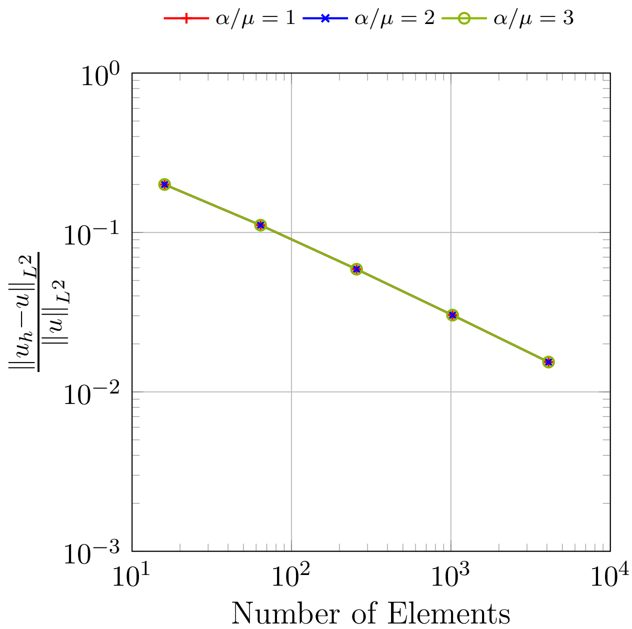

(b) Case two bubble function of which one mixed

Figura 4: The relative error versus the number of elements measured relative to the L^2 norm (regular mesh)

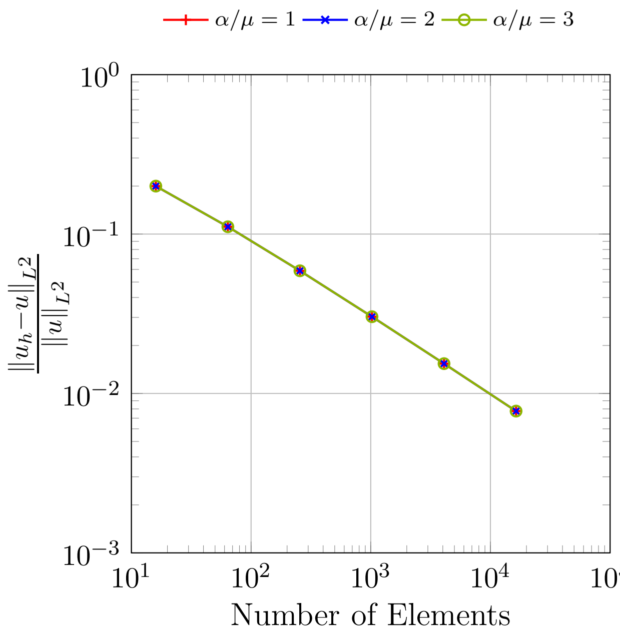

(a) type 1

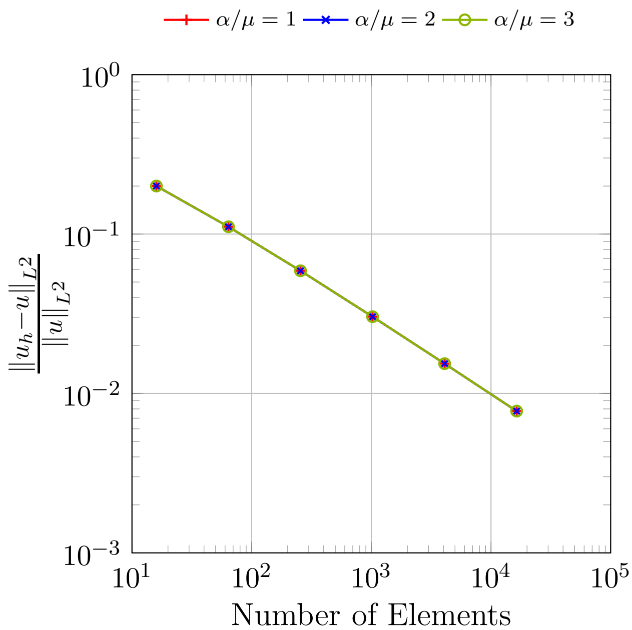

(b) type 2

Figura 5: The relative error vs. the number of elements measured relative to the L^2 norm (Case one bubble function and Trapezoidal mesh)

types of bubble functions used in the case of $\alpha/mu := 1, 2, 3$, while in figures 10(a), 10(b), 11(a) and 11(b) the same plots using trapezoidal meshes. In the all cases the elements distorted have a good behaviour respect to the regular mesh.

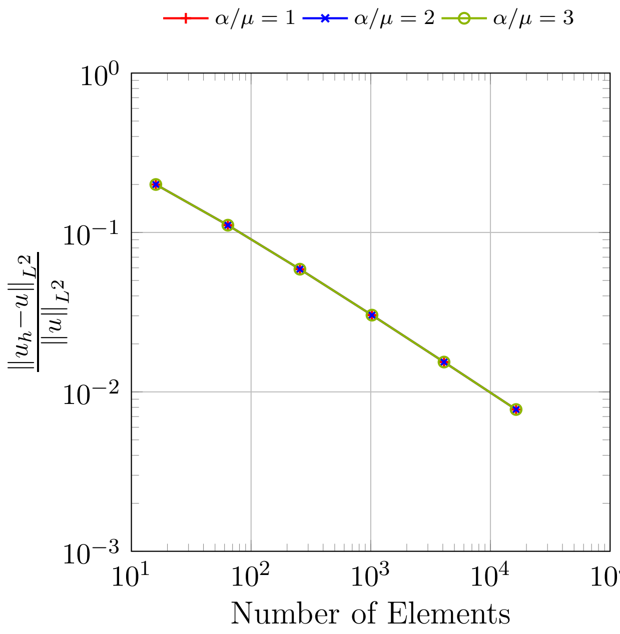

(a) Case two bubble function

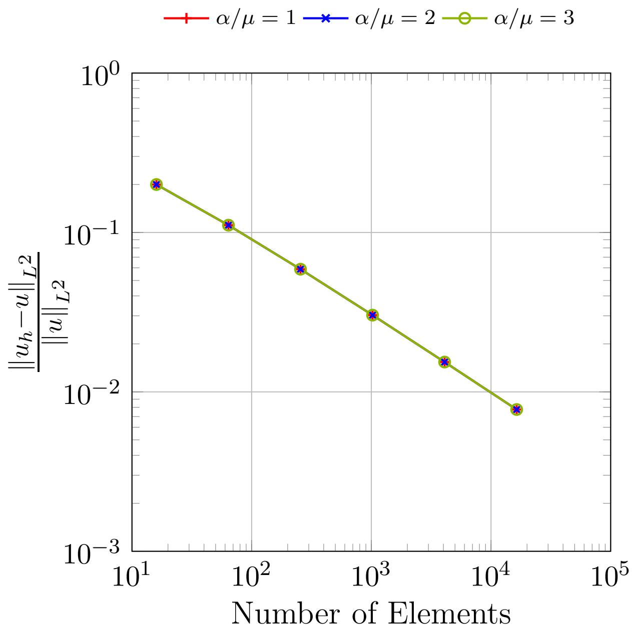

(b) Case two bubble function of which one mixed

Figura 6: The relative error vs. the number of elements measured relative to the L^2 norm (Case one bubble function and Trapezoidal mesh)

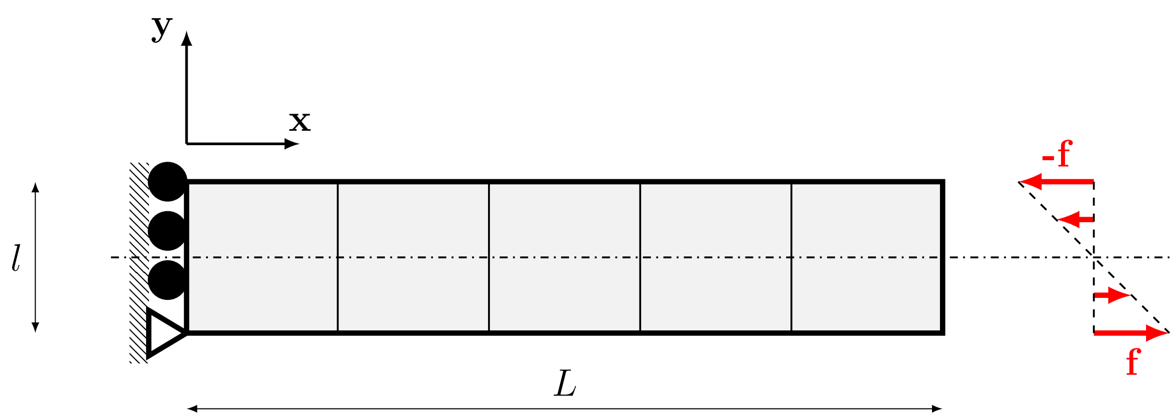

Figura 7: Beam cantilever geometry

5.3 Cook's membrane

The final example is the Cook's membrane. That is a typical benchmark and consist of a beam with vertex: $(0, 0)$, $(48, 44)$, $(48, 60)$ and $(0, 44)$. The left vertical edge is clamped and the right vertical edge subjected to the vertical distributed forces with resultant $F = 100$ as it shown in figure 12. The material properties are taken to be $E = 250$ and $\nu = 0.4999$, so that a nearly incompressible response is obtained. We report in figures 13(a), 13(b), 13(c) and 13(d) the vertical displacement of the point A versus the number of element per side for different choosing of the parameter $\alpha = \{1, \mu, 2\mu, 3\mu\}$. All elements return different behaviour using different coefficients α. In the case of $\alpha = 1$, figure 13(a), the obtained results completely not converge to the reference solution.

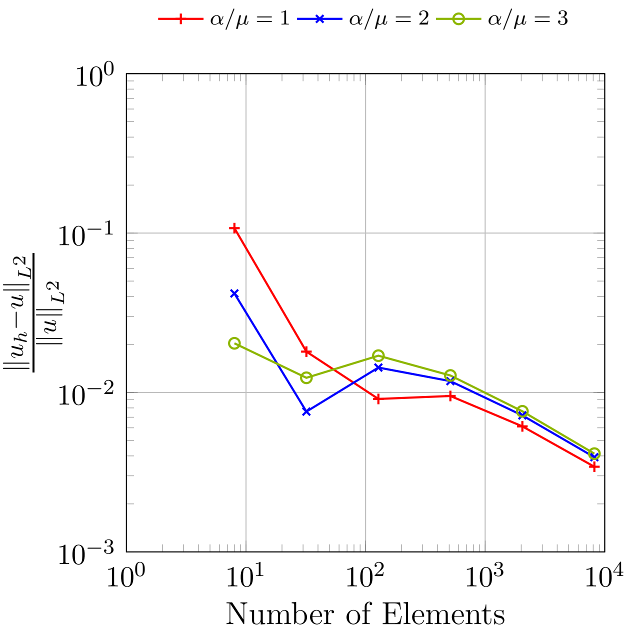

(a) Type 1

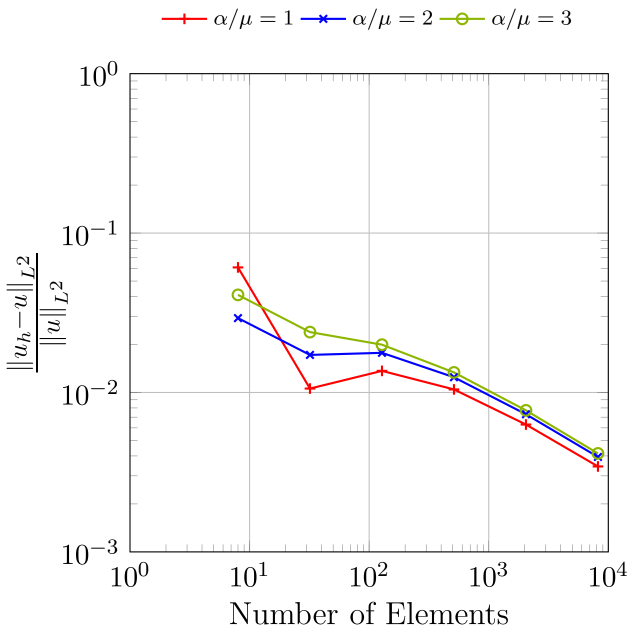

(b) Type 2

Figura 8: Beam Cantilever: the relative error vs. the number of elements measured relative to the L^2 norm (regular mesh)

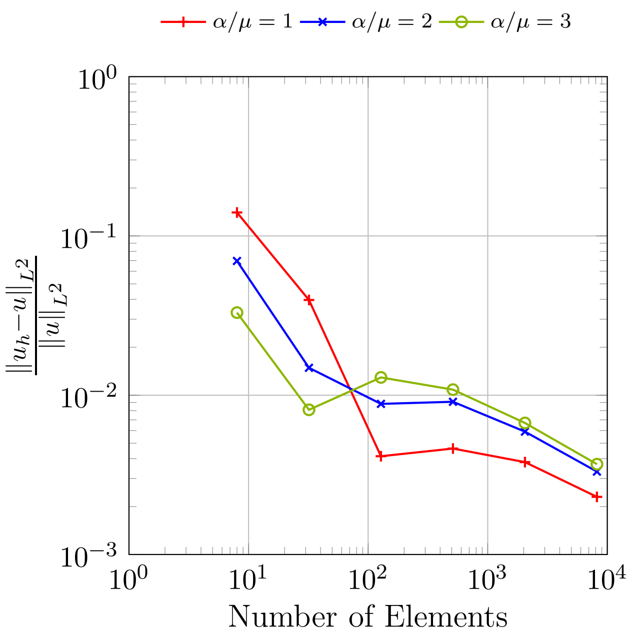

(a) Case two bubble function

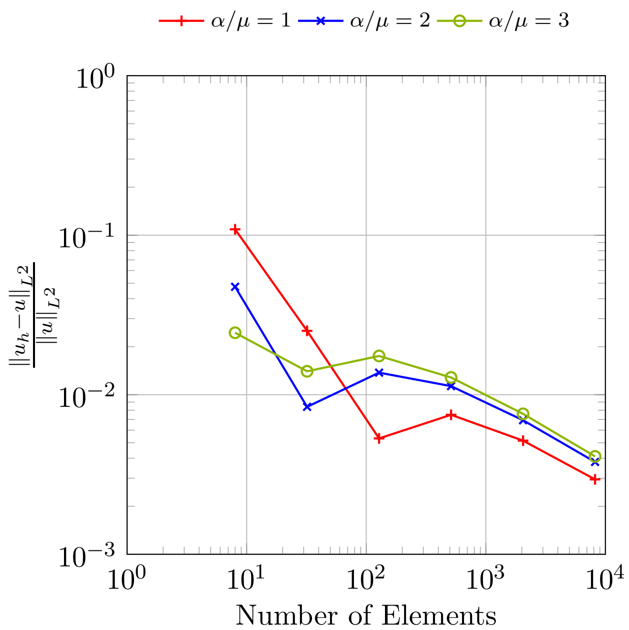

(b) Case two bubble function of which one mixed

Figura 9: Beam Cantilever: the relative error vs. the number of elements measured relative to the L^2 norm (regular mesh)

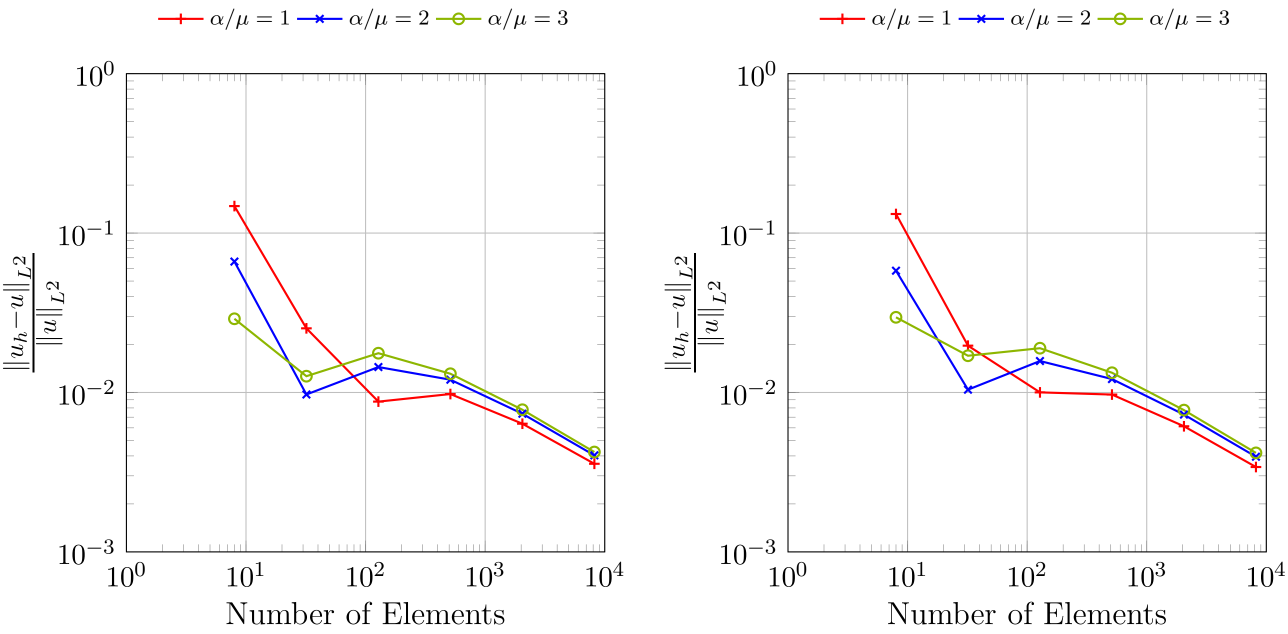

(a) Type 1

(b) Type 2

Figura 10: Beam Cantilever: the relative error vs. the number of elements measured relative to the L^2 norm (trapezoidal mesh)

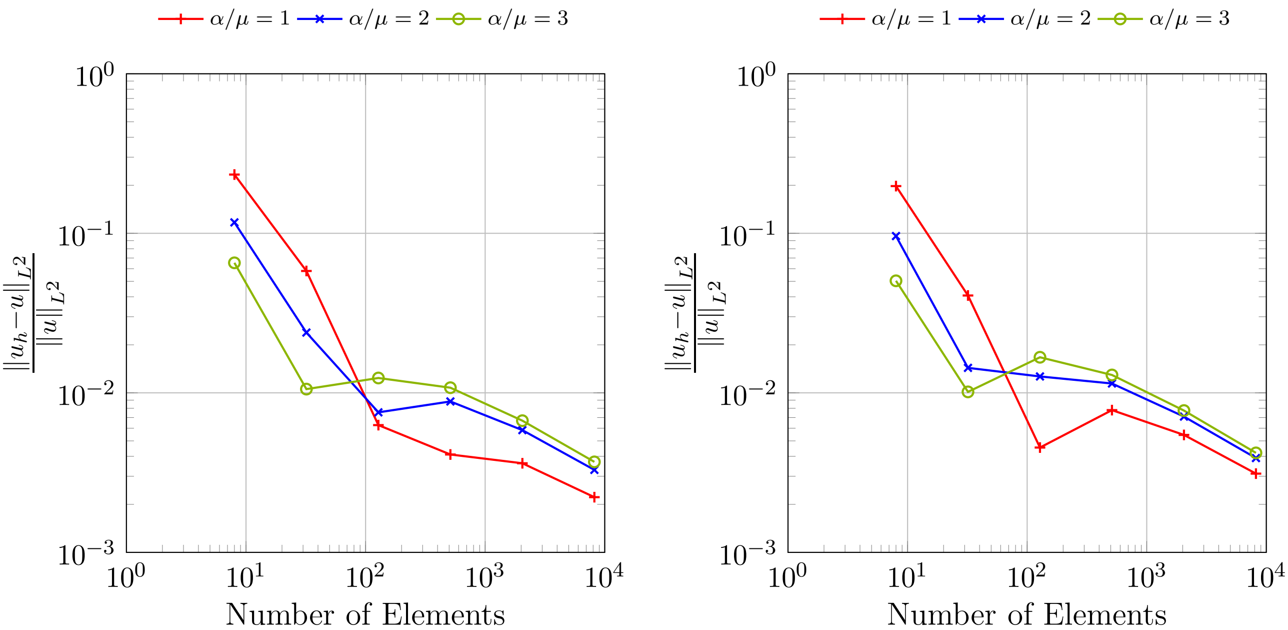

(a) Case two bubble function

(b) Case two bubble function of which one mixed

Figura 11: Beam Cantilever: the relative error vs. the number of elements measured relative to the L^2 norm (trapezoidal mesh)

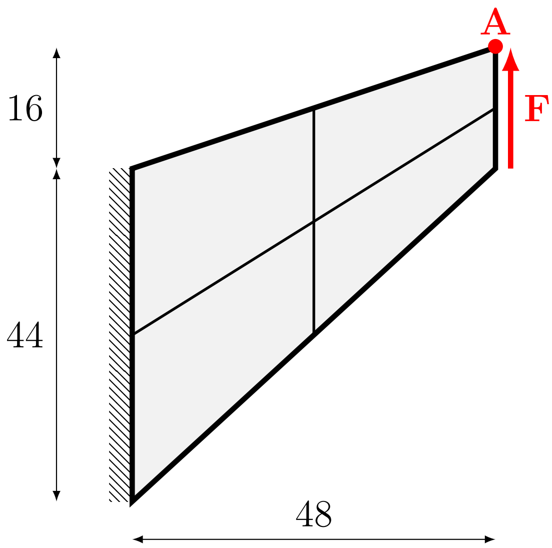

Figura 12: Cook's Membrane geometry

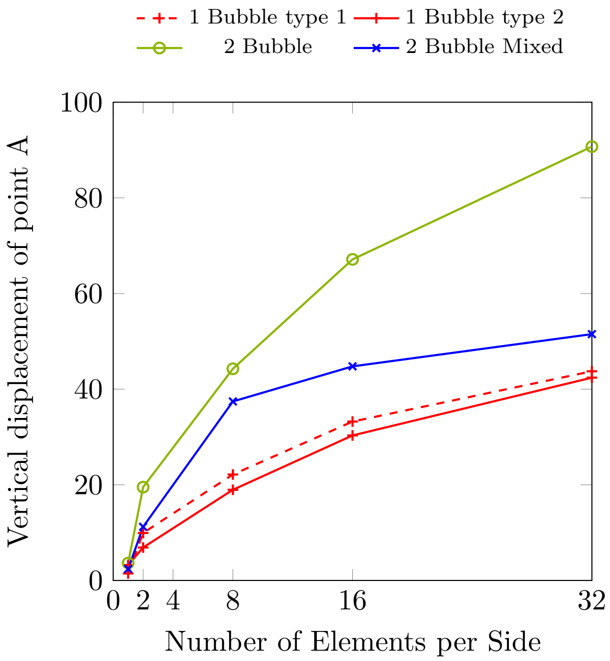

(a) $\alpha = 1$

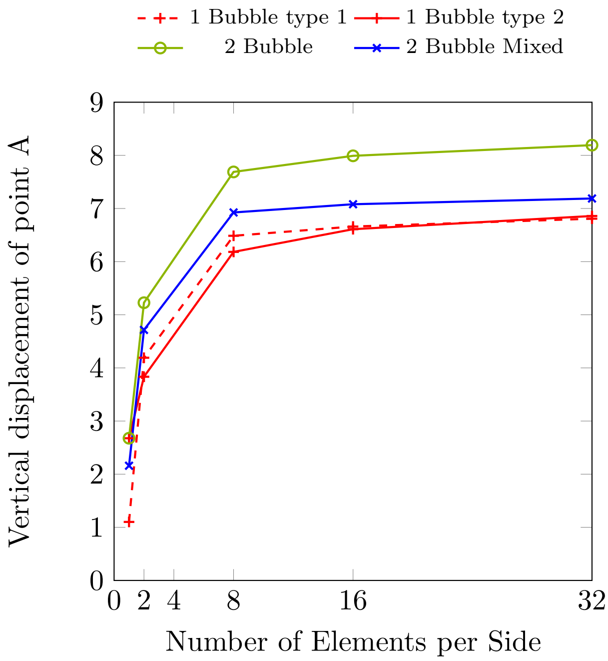

(b) $\alpha/\mu = 1$

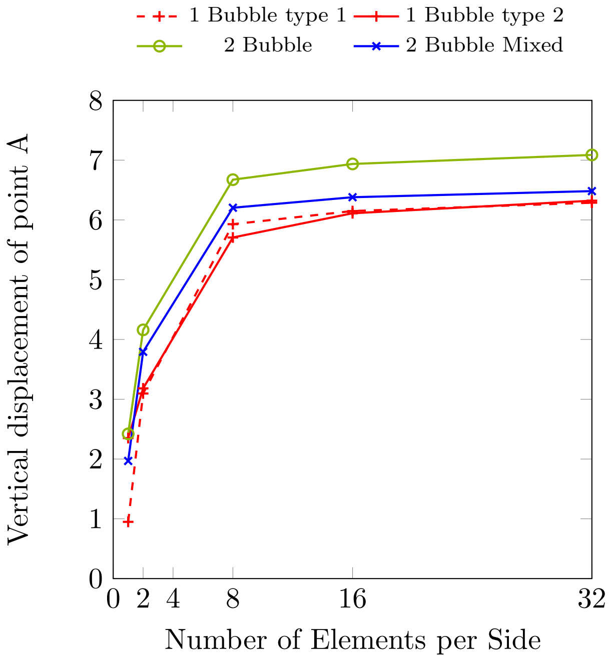

(c) $\alpha/\mu = 2$

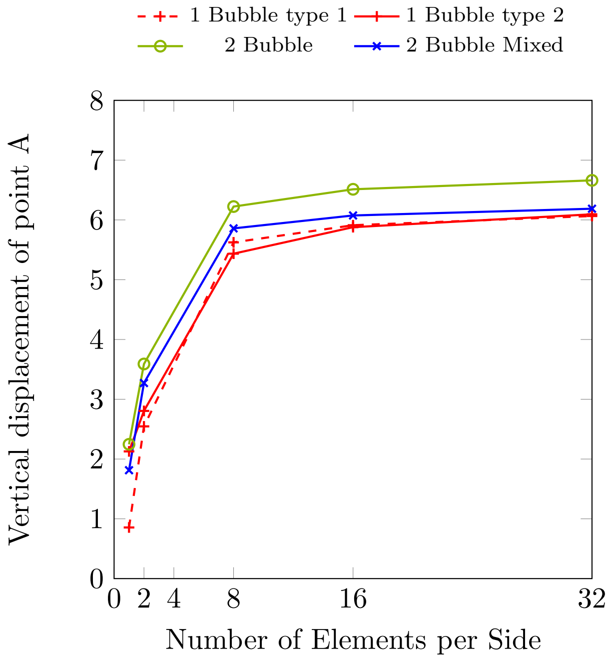

(d) $\alpha/\mu = 3$

Figura 13: Vertical Displacement of point A vs. the number of elements per side